ORIGINAL ARTICLE

Involvement of Rho kinase (ROCK) in sepsis-induced acute lung injury

Ismail Cinel[1,7], Mustafa Ark[2], Phillip Dellinger[3], Tuba Karabacak[5], Lulufer Tamer[6], Leyla Cinel[4], Paul Michael[9], Shaimaa Hussein[9], Joseph E. Parrillo[3], Anand Kumar[8], Aseem Kumar[9]

[1]Department of Anesthesiology & Reanimation Marmara University School of Medicine, Istanbul, Turkey; [2]Department of Pharmacology, Gazi University School of Pharmacy, Ankara, Turkey; [3]Department of Cardiovascular Disease and Critical Care Medicine, Division of Critical Care Medicine, Cooper University Hospital, Robert Wood Johnson Medical School, Camden, New Jersey, USA; [4]Department of Pharmacology; [5]Department of Pathology; [6]Department of Biochemistry, Mersin University School of Medicine, Mersin, Turkey; [7]Department of Anesthesiology& Reanimation Mersin University School of Medicine, Mersin, Turkey; [8]Section of Critical Care Medicine, University of Manitoba, Winnipeg, MB, Canada; [9]Department of Chemistry and Biochemistry and the Biomolecular Sciences Programme, Laurentian University, Sudbury, ON, Canada

ABSTRACT

Indirect acute lung injury is associated with high morbidity and mortality. We investigated the link between Rho kinase (ROCK) activation and apoptotic cell death in sepsis induced acute lung injury. This hypothesis was tested by administering a specific, selective inhibitor of ROCK (Y-27632) to rats subjected to cecal ligation and puncture (CLP). Rats were randomly divided into 4 groups as; sham-operated, sham + Y-27632, CLP and CLP + Y-27632. Twenty-four hours later, each experiment was terminated and lungs analyzed. Histopathology was assessed by hematoxylin-eosin staining and the presence of apoptosis was evaluated through the TUNEL assay. Pulmonary activity of caspase 3 and ROCK 1 & 2 were measured by western blot. Interstitial edema, severely damaged pulmonary architecture with massive infiltration of the inflammatory cells and an increase in lung tissue TBARS levels as well as 3-NT to total tyrosine ratios were observed in untreated CLP animals. Pretreatment of animals with Y-27632, reduced lung injury in the CLP induced septic rats in each of these parameters of lung injury (p<0.05). Western immunoblot revealed active caspase cleavage and increased expression of active fragment of ROCK 1 & 2 in the CLP group. TUNEL assay showed an increase in percentage of apoptotic cells when comparing the CLP group with the CLP + Y-27632 group. These results suggest an important role of Rho kinase in sepsis induced lung injury by a mechanism that might be related to oxidative and/or nitrosative stress mediated caspase cleavage leading to apoptosis.

KEY WORDS

Sepsis; acute lung injury; Rho kinase; ROCK; apoptosis; 3-Nitrotyrosine; peroxynitrite; reactive oxygen species; nitric oxide

Introduction

Severe sepsis and septic shock, associated with a mortality rate of 25-80%, are the leading causes of death despite recent advances in critical care medicine (1). A possible explanation for the ineffectiveness of traditional therapies may be the redundant and overlapping cellular signalling cascades initiated during sepsis (2,3). Recently, dysregulated apoptotic cell death has been proposed as a contributor to the morbidity and mortality in septic animals and patients (4,5). Indirect acute lung injury (ALI), caused primarily by nonpulmonary sepsis, represents a primary event which may signal the onset of widespread multi-organ dysfunction syndrome (MODS) (6). Activation of apoptotic signalling appears to be a relevant and early event in the development of indirect ALI (7). Lung epithelial and endothelial barrier dysfunction, potentially related to apoptosis, is critical to the edema formation and pathologic derangement observed in sepsis-induced acute lung injury (8,9). However, a detailed cellular mechanism still remains to be elucidated.

Rho is a small GTPase and reported to be the molecular switch for intracellular signalling (10). Numerous effector molecules of rho have been identified, among which two serine/threonine kinases, rock-I and rock-II, are frequently reported

(11). Rho kinases are composed of NH2-terminal catalytic, coiled coil, rho binding, and COOH-terminal pleckstrin-homology domains (12). These kinases phosphorylate various substances, including myosin light chain phosphatase and mediate the formation of actin stress fibers and focal adhesions in various cell types. These molecules are involved in many aspects of cell motility which include smooth muscle cell contraction and cell migration (13,14). Pharmacological manipulation of this pathway can be achieved with agents such as clostridium botulinum toxin C3, which inhibits small GTPase rho, or fasudil or Y-27632 that specifically inhibit its effector rho kinase (13). Reorganisation of the endothelial cytoskeleton, which include actin filaments, microtubules and intermediated filaments, leads to alteration in cell shape and provides a structural basis for increase of vascular permeability. This process has been implicated in the pathogenesis of pulmonary endothelial barrier dysfunction in acute lung injury. Tasaka *et al.* (14) has suggested an important role of rho GTPase-mediated signalling in the endotoxin-induced acute lung injury. However, an in vivo model and investigation of detailed mechanism of action are required to define the role of rho/rho kinase in sepsis-induced lung injury.

It has been shown that the rho/rho kinase pathway is involved in the mechanisms of apoptosis (15,16). Shiotani *et al.* (17) have demonstrated that rho kinase-mediated production of reactive oxygen species (ROS) and inflammatory cytokines are substantially involved in the pathogenesis of ischemia reperfusion injury. Although it has been demonstated that rho kinase regulates the production of ROS through activation of an NADPH oxidase in neutrophils, it is unknown whether Rho kinase is involved in sepsis-induced ROS and reactive nitrogen species (RNS) production and tissue injury in vivo (18,19). It has been shown that rho effector protein ROCK 1 is cleaved during apoptosis to generate a truncated active form (20,21). Furthermore, direct cleavage of ROCK 2 by granzyme B defined ROCK 2 as the inducer of apoptotic membrane blebbing in a caspase-independent manner in several cell lines (22). In a parallel manner, we have also shown the fragmentation of ROCK 2 in human placentas from preeclamptic patients (23). However, there has been no report documenting this pathway in an animal model of sepsis.

In the present study, we examined the effects of a specific, selective inhibitor of ROCK, Y-27632 on oxidative and nitrosative damage and apoptotic cell death in rat lungs in a cecal ligation and puncture (CLP)-induced sepsis model. Control groups of sham and untreated CLP were also utilized for comparison. Lung injury was evaluated biochemically, histopathologically and immunhistochemically in lung sections. Pulmonary activity of caspase 3 and ROCK 1 & 2 were measured by western blotting and apoptosis was measured by tunel assay. Edema was assessed with wet/dry (W/D) lung ratios and inflammation was assessed in bronchoalveolar fluid (BALF).

Contribution of oxidative and nitrosative stress was assessed by measuring the levels of thiobarbituric acid reactive substances (TBARS) and 3-L-nitrotirozin (3-NT) /total tyrosine ratio (an indicator of the formation of peroxynitrite) in lung homogenates.

Materials and methods

The experiments described in this article were performed in adherence with National Institutes of Health Guidelines on the use of experimental animals. Our study was approved by the animal ethics commitee of the School of Medicine, Mersin University. Sixty, male, Wistar rats, weighing between 220-250 g were housed at constant temperature with 14/10h periods of light and dark exposure, respectively. Animals were allowed access to standard rat chow and water ad libitum and acclimatized for at least one week prior to use in these experiments.

Experimental sepsis by CLP: Anesthesia was induced by intramuscular (i.m.) administration of ketamine 50 mgkg^{-1}, and xylazine 7 mgkg^{-1}. After shaving the abdomen and application of a topical disinfectant, a two cm midline incision was made below the diaphragm to expose the abdominal organs. After the identification of the cecum, it was ligated below the ileocecal valve without occluding the bowel passage. The cecum was then subjected to a single "through and through" perforation with an 18-gauge needle distal to the point of ligation. The needle was removed and a small amount of stool was extruded from both punctures to ensure potency. After repositioning the bowel, the abdominal incision was closed with 4/0 sterile synthetic absorbable suture (Polyglactin 910, Vicryl, Ethicon Ltd., Edinburg) and the skin clips (Ethicon, Somerville, NJ). Sham-operated animals underwent the same procedure except for ligation and puncture of the cecum.

Experimental Protocol: After fasting overnight, 60 rats were randomly divided into four groups. The first group (sham group, n=15) served as sham-operated and the third group (CLP group, n=15), was subjected to cecal ligation and puncture (CLP). The second group (sham + Y27632 group, n=15) and the fourth group (CLP + Y-27632, n=15) were given (+)-(R)-trans-4-1-aminoethyl-N-4-pyridyl cyclohexane carboxamide dihydrochloride monohydrate (Y-27632, a selective ROCK inhibitor) 1.5 mgkg-1 intraperitoneally (i.p.) 20 min prior to sham or CLP operations. All animals received fluid resuscitation. Twenty four hours later, rats were anesthetized with i.m. ketamine 80 mgkg^{-1}. After mid-line sternotomy, blood samples were taken with cardiac puncture and the right bronchus was clamped. Bronchoalveolar lavage of the left lung was performed with 2 ml of saline and then both lungs were harvested. Right lung was divided into four equal parts. To evaluate the CLP-induced lung injury one part was fixed in 10% formaldehyde and the other was preserved for W/D weight ratios. The final

two parts were taken for biochemical assay and Western blot. Lung specimens were kept frozen at -70°C until analysis. BALF was used for measurement of infiltrating cells and protein concentrations.

The determination of thiobarbituric acid reactive substances: Tissue was homogenized in 10 parts 15 mmol/L KCL for thiobarbituric acid reactive substances (TBARS) assay. The TBARS levels, an index for lipid peroxidation, was determined by thiobarbituric acid reaction described by Yagi (24). The principle of the method is based on spectrophotometric determination of the intensity of the pink color produced by interaction of the barbituric acid with malondialdehyde liberated as a result of lipid peroxidation. We used 1,1,3,3 tetraetoxypropane as the primary standard.

The determination of 3-nitrotyrosine/total tyrosine ratio: For tyrosine assay lung tissue was homogenized in ice-cold phosphate buffered saline (pH=7.4). Equivalent amounts of each sample were hydrolyzed in 6N HCl at 100°C for 18-24h, samples were then analyzed on a HP 1049 HPLC apparatus. The analytical column was a 5 μm pore size Spherisorb ODS-2 C_{18} reverse-phase column (4, 6-250 mm; Alltech, Deerfield, IL, USA). The guard column was a C_{18} cartridge (Alltech). The mobile phase was 50 mmoL l^{-1} sodium acetate/50 mmoL l^{-1} citrate/8% methanol, pH=3.1. HPLC analysis was performed under isocratic conditions at a flow rate of 1 ml min^{-1} and the UV detector was set at 274 nm. 3-nitrotyrosine (3-NT) determination was made by comparison of the sample's peak area with the peak area produced by the external standard solution of 10 μmolL^{-1} 3-NT (25). The results were expressed as 3-NT / total tyrosine ratio.

Lung wet-to-dry weight ratio: Lung wet-to-dry (W/D) weight ratios were used as a measure of pulmonary edema. The W/D weight ratio of the left lung was calculated by weighing the freshly harvested organ, and then heating it at 90°C in a gravity convection oven for 72 hours to attain its dry weight (26).

Number of Infiltrating Cells and Protein Concentration in BALF: The number of infiltrating cells and the protein concentration in BALF were used as indicators of the degree of lung inflammation. BALF samples were stored in ice water until testing. Cell counts and total protein concentrations were measured on the day of sample collection. For cell counting, 1μl of bronchoalveolar aspirate was placed on a glass slide, air-dried, and then stained by modified Giemsa's method. The total number of inflammatory cells (polymorphonuclear leukocytes-[PMNs]) in each 1 μl sample was then counted under the light microscope by a pathologist unaware of the groups. The remainder of the bronchoalveolar fluid was preserved for analysis of protein content. The total protein concentration in a bronchoalveolar fluid sample was measured using the method of Lowry *et al.* (27).

Histopathological Examination: The specimens were fixed in 10% formalin for 24h, and standard dehydration and paraffin-wax embedding procedures were used. H&E-stained slides were prepared by using standard methods. Light microscopic analyses of lung specimens were done by blinded observation to evaluate pulmonary architecture, tissue edema formation and infiltration of the inflammatory cells as previously defined (9). The results were classified into four grades where Grade 1 represented normal histopathology; Grade 2 indicated minimal neutrophil leukocyte infiltration; Grade 3 represented moderate neutrophil leukocyte infiltration, perivascular edema formation and partial destruction of pulmonary architecture and finally Grade 4 included dense neutrophil leukocyte infiltration, abcess formation and complete destruction of pulmonary architecture.

TUNEL Assay: TUNEL assay was performed on paraffin embedded lung tissues from Sham, CLP and CLP + Y-27632 groups. Sections 5 μm thick were mounted on subbed slides, deparaffinized at 57 °C for 5 minutes on a slide warmer then immersed in 2 changes of mixed xylenes 5 minutes each. The sections were hydrated by immersing them in an alcohol series ranging from 100% to 70% ethanol. This was followed by 2 washes in PBS 5 minutes each. The staining of the sections was performed according to R&D systems Tacs TdT In Situ Apoptosis Detection kit (TA4626). Briefly sections were permeabilized with proteinase K at 37 °C for 22 min. This was followed by quenching of endogenous peroxidases by treating the sections with a 3% hydrogen peroxide solution for 5 minutes. The labelling reaction with biotinylated dNTPs was incubated for 2 hours at 37°C in a humidified chamber. Detection was performed by using streptavidin conjugated to HRP at double the concentration for 10 minutes at room temperature. The addition of Tacs blue for 5 minutes to each section was followed by 3 washes in water. The sections were counterstained with nuclear fast red, had coverslips mounted with Permount® (FisherScientific) and documented with a Ziess Axiovert 200M deconvolution microscope. Five fields of view for each section were counted using the 40X objective and the number of blue cells expressed as a percent of the total cell number was averaged over the 5 fields to give the percent of apoptotic cells per treatment.

Western Blot: Western blot experiments were performed as previously described (28). In brief, lung tissues were homogenized in cold buffer containing 50 mM Tris-HCl (pH 7.5), 400 mM NaCl, 2 mM EGTA, 1 mM EDTA, 1 mM DTT, 10 μM PMSF, 10 μg ml^{-1} leupeptine, 1 μg ml^{-1} pepstatin and 1mM benzamidine. Nuclei and unlysed cells were removed by low speed centrifugation at 900 x g, 4°C for 10 min. Protein concentration of supernatant was determined by Lowry method. The supernatant (200 μg of protein) was mixed with an equal volume of 2x SDS sample buffer and boiled for 5 min. Proteins were separated by SDS polyacrylamide gel electrophoresis (8 % acrylamide) and blotted onto a PVDF membrane. Membranes

were blocked for 1 h with 5 % (w/v) dry nonfat milk in TBS-tween. Blots were then incubated in mouse monoclonal anti-Rock 1 and anti-Rock 2 antibody which detects both active and inactive forms of Rocks (1:500, Transduction Laboratories) actin (1:500, LabVision) and caspase 3 which only detects 19 and 17 kDa fragment of caspase 3 (1:1000, Cell Signalling) for 3 h. An HRP-conjugated secondary antibody was used in conjunction with an enhanced chemiluminescence detection kit (ECL Plus) from Amersham Pharmacia Biotech to visualize the immunopositive bands on X-ray film. Equal protein loading was verified using actin antibody and coomassie brillant blue (cbb) staining of membranes. The intensities of the bands were quantified by densitometry using Scion image computer program (Scion Corp. Beta 4.0.2). Percent fractionation of ROCK 1 and 2 was calculated by the following equation;

% Fraction of rock 1 or 2 = [ODact x 100] / [ODact + ODinact]

ODact : Optic Density of active fragment.

ODinact : Optic Density of inactive fragment.

Statistical Analysis: Biochemical values are given as mean ± SEM values. Statistical differences for protein concentration and number of inflammatory cells in BALF, TBARS, 3-nitrotyrosine/total tyrosine ratio, wet to dry weight ratio and TUNEL cell counts in lung specimens were evaluated using one-way analysis of variance followed by Tukey test. Comparison of total lung injury and caspase 3 staining scores were analyzed using Kruskall-Wallis variance analysis followed by Dunn test. *p* values less than 0.05 were considered significant.

Results

All animals in the sham-operated, sham + [Y-32627] and CLP + Y-27632 groups survived the experimental period. Four rats in the CLP group died during the last two hours of the 24 hour period.

Lung Tissue TBARS levels

The levels of TBARS in lung tissue is demonstrated in Figure 1A. Lung tissue TBARS levels were significantly increased in the CLP group in comparison to the sham-operated group. Y-27632 treatment prevented the increase in lung tissue TBARS levels in comparison to the CLP group. The suppression of TBARS level was accompanied by attenuated polymorphonuclear neutrophils and lung injury scores in sections of histopathologic assesment (Figure 2A and 3).

Lung Tissue 3-nitrotyrosine/total tyrosine ratios

Lung tissue 3-NT/total tyrosine ratios are demonstrated in Figure 1B. In the CLP group lung tissue 3-NT/total tyrosine ratio was significantly increased whereas Y-27632 was associated with a lesser CLP-induced increase in 3-NT/total tyrosine ratio.

Lung Tissue Wet-to-dry Weight ratios

The wet-to-dry (W/D) weight ratio, a parameter of pulmonary edema, increased significantly in the CLP group in comparison to the sham-operated group (Figure 1C). This increase was significantly reduced in the Y-27632 + CLP group. Treatment with Y-27632 alone did not cause lung edema.

Number of Inflammatory Cells and Protein Concentrations in Bronchoalveolar Lavage

The number of inflammatory cells in BALF at 24 hours increased significantly in the CLP group when compared with sham-operated group. This increase in the number of inflammatory cells was significantly reduced in the CLP + Y-27632 group (Figure. 2A). Similarly, BALF protein concentrations markedly elevated in the CLP group compared with the sham group, whereas the elevation was significantly attenuated in the CLP + Y-27632 group (Figure 2B). Y-27632 treatment alone did not cause significant changes in number of inflammatory cells and protein concentrations in BALF from sham treated rats. In the sham group, a trace amount of infiltrating cells were detected in the BALF and were similar to findings with sham + Y27632 treatment.

Light Microscopy Findings

There were no significant light microscopic differences between lungs of sham and sham + Y-27632 group. In the CLP group, interstitial edema with massive infiltration of the inflammatory cells into the interstitium and alveolar spaces were observed and the pulmonary architecture was severely damaged. These morphologic changes were less pronounced in the CLP + Y-27632 group and pulmonary architecture was preserved and lung injury score was reduced in the sham + Y-27632 group (Figures 3 and 4 A, B, C). TUNEL assay showed CLP + Y-27632 contained less apoptotic cells then the CLP group (Figures 5 A,B,C). CLP + Y-27632 had a mean percent of 7.0 ±1.5 apoptotic cells while the CLP group had a mean percent of 17.8±2.2 apoptotic cells (Table 1). The sham group had no detectable apoptotic cells (Figure 5A).

Western Blot Experiments in Lung Homogenates

These experiments were designed to evaluate ROCK 1 and 2 protein expressions and possible active fragmentations (130 kDa) of these rock isoforms in control and CLP rat lung tissues. As shown in figure 6A and B, increased active fragmentation of
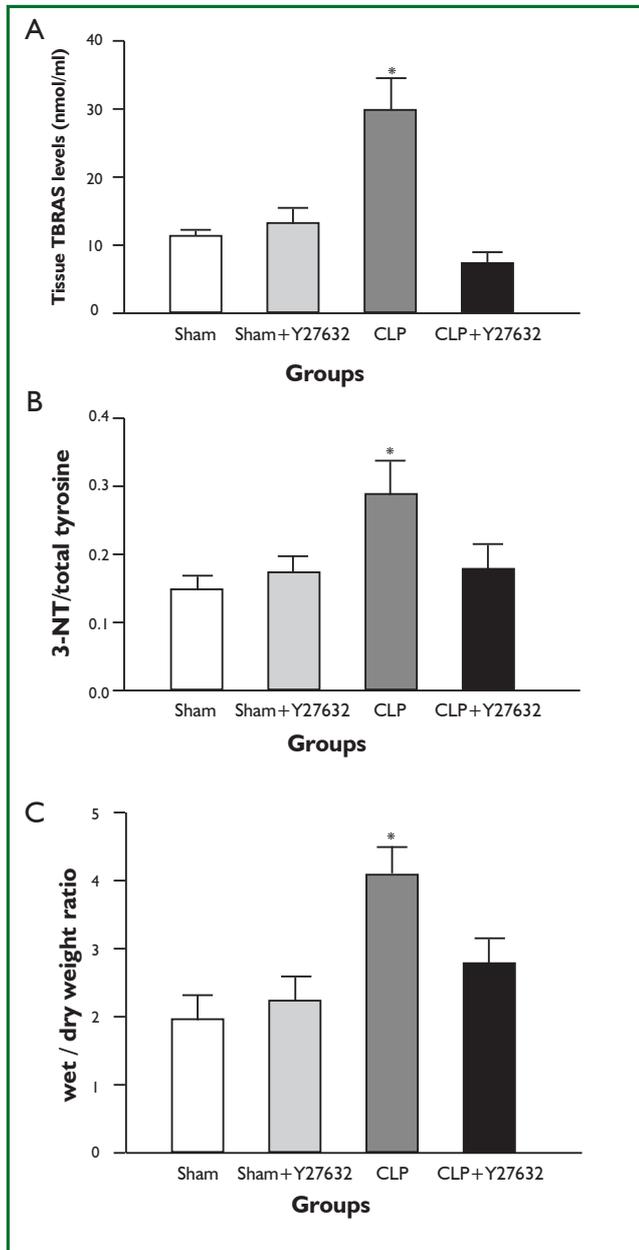
Figure 1. Lung tissue TBARS levels, 3-Nitrotyrosine/Total Tyrosine Ratio and Wet to Dry Weight Ratio (W:D). A: CLP resulted in increased lung TBARS levels compared with the sham operated animals. The CLP-induced increase was reduced by Y-27632 treatment; B: CLP increased 3-nitrotyrosine/Total Tyrosine ratios and Y-27632 prevented these increases; C: Lung tissue W/D weight ratios were significantly increased in CLP group in comparison to sham-operated group. Y-27632 treatment caused significant decrease in the W/D weight ratio in comparison to CLP group. All data represent mean±S.E.M.; For comparison analysis of variance (ANOVA) followed by Tukey post hoc test was used. *P<0.05 compared with the other groups.
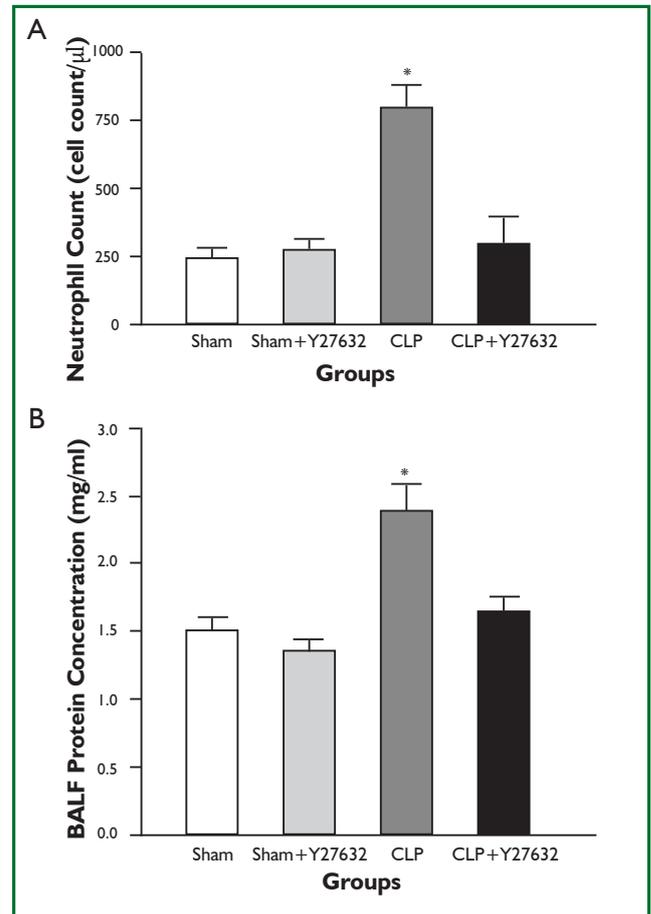
Figure 2. Number of Inflammatory Cells and Protein Concentrations in Bronchoalveolar Lavage Fluid. A: In the CLP group, cellular infiltration in the BALF was found to be increased when compared with sham-operated group, whereas Y-27632 treatment in CLP group caused decrease in cellular infiltration in the BALF compared to the CLP group; B: In the CLP group, protein concentrations in the BALF was found to be increased and Y-27632 prevented these increases. All data represent mean±S.E.M.; For comparison analysis of variance (ANOVA) followed by Tukey post hoc test was used. *P<0.05 compared with the other groups.

Table 1

Treatment	% apoptotic cells(Mean ± SEM)
Sham	0
CLP+Y27632	7.0±1.5*
CLP	17.8±2.2*

* P<0.05 SEM standard error of the mean. p value determine by one way ANOVA. Percentage apoptotic cells determined by TUNEL assay. Sample means are derived from counts from 5 fields of view per section per group at 400X magnification.
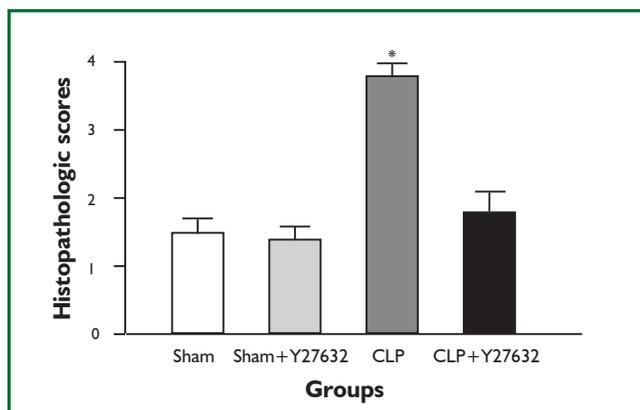
Figure 3. Histopathological scores of the Lung Tissues.
Histopathological scores of the lung tissue. CLP resulted in increased lung histopathologic scores compared with sham-operated animals. The CLP induced increase was reduced by Y-27632 treatment. For comparison Kruskall-Wallis variance analysis followed by Dunn test was used. *P<0.05 compared with other groups.

both rock isoforms were detected in CLP treated lung tissues. We also evaluated caspase 3 fragmentation in lung tissues. Compatible with our rock cleavage findings, we found increased caspase 3 17 kDa active form in the CLP rat lung tissues Figure 6C.

Discussion

Although multiple mechanisms such as increased permeability, polymorphonuclear leukocytes recruitment and inflammation have been implicated in the pathogenesis of non-pulmonary sepsis-induced acute lung injury, its detailed cellular mechanisms remain poorly characterized. In the present study, we have demonstrated that sepsis induces active fragmentation of ROCK 1 & 2 and caspase 3 cleavage associated with apoptosis in lung tissue. Interstitial edema severely damaged pulmonary architecture with massive infiltration of the inflammatory cells and an increase in lung tissue TBARS levels and 3-NT to total tyrosine ratio and apoptotic cells were observed in untreated CLP animals. Pretreatment of animals with a specific rho-kinase inhibitor, Y-27632, reduced lung injury in this clinically relevant model of sepsis. These findings demonstrate the role of rho kinase in the pathogenesis of sepsis-induced lung injury, and the ability of rho kinase inhibitor to reduce lung injury. The results of the study suggest that activation of ROCK 1 & 2 are involved in the pathogenesis of sepsis-induced ROS and/or RNS-mediated, apoptosis-related acute lung injury.

The transendothelial migration of neutrophils is a critical step in inflammation and the role of infiltrating PMNs, ROS and/or RNS in sepsis induced organ damage is well established. Recent studies suggest that rho and rho kinase are key mediators of myosin light chain (MLC) phosphorylation and have important roles in neutrophil migration (29,30). Endothelial rho and rho kinase regulate transendothelial neutrophil migration by modulating the cytoskeletal events that mediate such migration (14,30). In our study, the increased levels of inflammatory cell counts in BALF and increased levels of lung tissue TBARS and 3-NT/total tyrosine ratio (a marker of peroxynitrite formation) indicate that leukocyte recruitment and oxidative and/or nitrosative stress are induced after CLP. Histopatologic data showing edema and leukocyte infiltration in lung tissues obtained from the CLP group support these biochemical changes. The demonstration of rho kinase-mediated leukocyte infiltration in endotoxemic liver injury and ROS production in I/R injury are also in concordance with our results (17,31). Another finding of this study is the simultaneous suppression of TBARS and 3-NT/total tyrosine ratio by Rho kinase inhibitor, Y-27632, preventing not only oxygen centered free radical damage but also peroxynitrite mediated lung injury. No evidence of Y-27632 antioxidant activity in vitro has been reported, thus the fact that Y-27632 can protect cells from lipid peroxidation in this study may result from its antiinflammatory activity rather than from its direct antioxidant activity.

Microfilaments and cytoskeletal actin are the major structures involved in maintaining cell shape. Gaps between endothelial cells open in inflammation which may lead to extravasation of fluid and macromolecules. Involvement of rho kinase in neutrophil-stimulated endothelial hyperpermeability, microvascular leakage and lung microvascular permeability has been demonstrated (28,32,33). Alveolar epithelium can also contribute to inflammation by releasing inflammatory mediators which is governed by rho signalling (34). Zeng *et al.* (35) studied the effect of recombinant human activated protein C on endothelial cell permeability and modulation of the intracellular cytoskeleton via rho kinase pathway to reveal clinically improved organ function. Our CLP model was associated with significant capillary leak and lung edema, as evidenced by increased protein in the BALF and increased W/D ratio. Pretreatment with Y-27632 significantly decreased BALF proteins and lung edema. The decrease in edema formation and amelioration of lung damage suggests that Rho kinase inhibition prevents the activation of neutrophil-dependent oxido-inflammatory pathways and thus contributes to the reduction of fluid extravasation and improved histopathology. Supporting our results, it has been shown that Rho and Rho kinase are involved in neutrophil stimulated increase in endothelial permeability and in cytokine-mediated barrier dysfunction in the pathogenesis of pulmonary edema associated with acute lung injury (28,32,33,36,37). The importance of rho kinase pathway in ROS, specifically H_2O_2-induced pulmonary edema has been described in one previous study (38). Our study suggests an additional role of RNS in the rho kinase related lung edema. In addition, a recent study demonstrated that rock inhibitor,
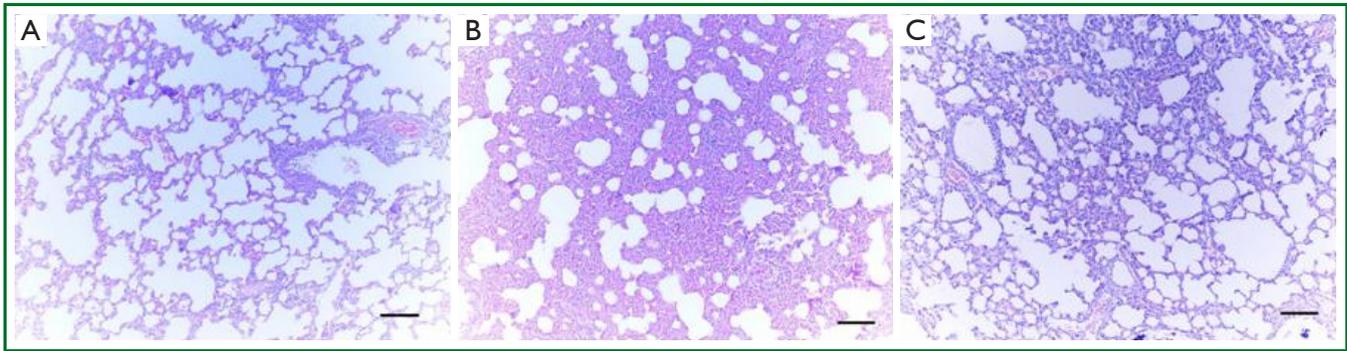
Figure 4. Photomicrographs of Lung Tissues (Hematoxylin & Eosin X100). A: Normal pulmonary histology was observed in sham group (grade 1); B: CLP group revealed severe interstitial infiltration of neutrophils and destructed pulmonary architecture (grade 3); C: In the CLP + Y-27632 group, there was improvement of the deranged histopathology observed in CLP Group (grade 2).
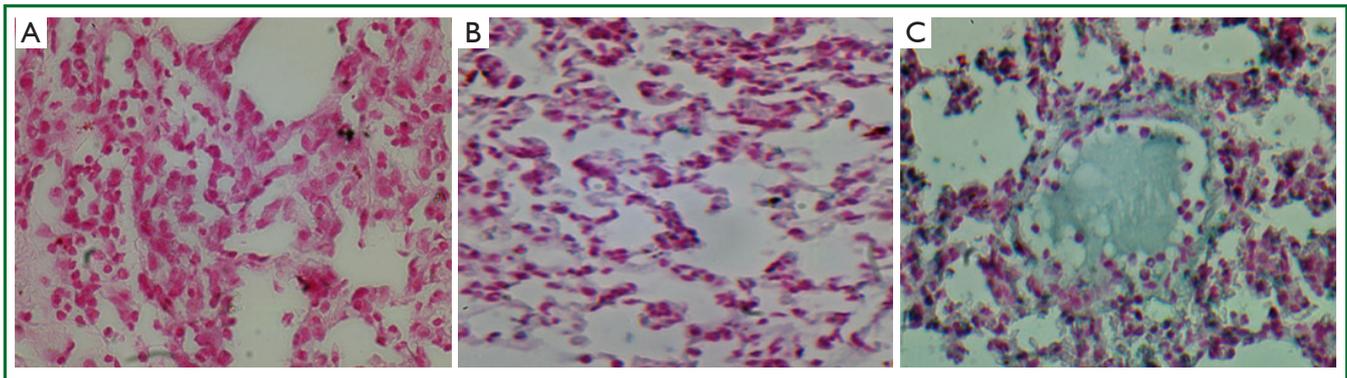
Figure 5. Photomicrographs of Lung Tissues (Tunel Assay X400). A: Sham group 5 μm section stained with Tacs Blue and Nuclear Fast Red; B: CLP + Y-27632 group 5 μm section stained with Tacs Blue and Nuclear Fast Red; C: CLP group 5 μm section stained with Tacs Blue and Nuclear Fast Red.

Y-27632, prevented the TNF-α related increased permeability in a lipopolysaccharide (LPS) model (14). Rho kinase inhibitors are also defined as a potent inhibitor of TNF-α and chemokines in bronchial epithelial cells and may be an additional therapeutic option in sepsis (38). Contrary to our findings, Lundblad *et al.* (40) has reported the permeability-reducing effects of prostacyclin and stated that inhibition of Rho kinase did not counteract endotoxin-induced increase in permeability in cat skeletal muscle. The different findings between the two studies may be attributed to the selection of different animal models and organs such as cat skeletal muscle in LPS induced-endotoxemia versus rat lung in CLP-induced sepsis.

Peroxynitrite has been identified as a noxious stimulus for lung inflammation (25,41). Peroxynitrite is known to induce DNA laddering and caspase 3 activation in different cell types including human endothelial cells in cultures (42,43). On the other hand, it has been recently shown that rock 1 cleavage, which produces the 130 kDa active form of the enzyme, requires caspase 3 activation (44). There is increasing appreciation that the microfilamentous cytoskeleton may be intrinsically involved

in the cell damage by regulating intracellular signaling or by transmitting death messages to downstream effectors. This is the first in vivo study which shows ROCK 1 & 2 fragmentation response to sepsis. It can be assumed that rho kinase may be required for membrane blebbing in apoptosis induced by peroxynitrite. In this study, rho kinase appears to have a critical role in indirect acute lung injury in sepsis. Inhibition of rho kinase pathway prevented the increase in peroxynitrite levels in lung tissue which was associated with a decrease in the number of apoptotic cells in the CLP + Y-27632 group. Of note, Thorlacius *et al.* have demonstrated the protective effect of Y-27632 on apoptosis in LPS induced liver injury (31). It is possible to postulate the following vicious cycle in sepsis: rho kinase activation is associated with increased epithelial permeability and followed by leukocyte migration and neutrophil infiltration with the consequence of production of ROS and peroxynitrite which triggers caspase cleavage and so rho kinase activation again. Lending support to this hypothesis, one recent study has demonstrated the involvement of peroxynitrite in caspase-3 mediated apoptosis at the tissue level (45). In addition 3-NT,
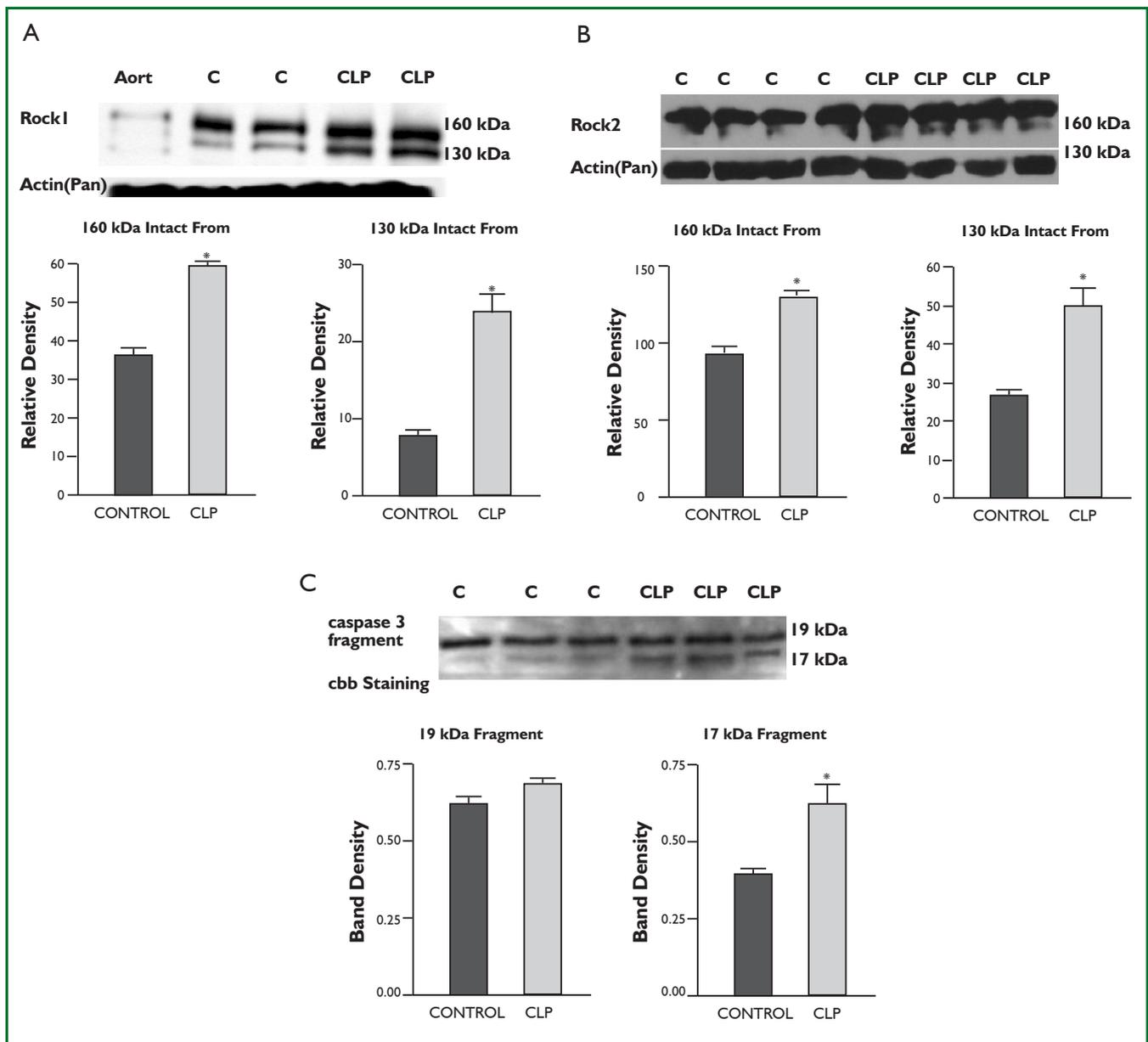
Figure 6. Western Blot findings in Lung Homogenates from Sham operated and CLP rats. A: The homogenates were subjected to SDS gel electrophoresis and transferred to PVDF membranes, which were incubated with specific antibody against ROCK 1; B: The same as A. except that ROCK 2 antibody was used; C: The homogenates were subjected to SDS gel electrophoresis and transferred to PVDF membranes, which were incubated with specific antibody against 19/17 kDa fragment of caspase 3. Sham-operated lung homogenate, CLP: CLP lung homogenate, Cbb: Coomassie brillant blue. See Methods section for details.

as a marker of peroxynitrite production, is also increased in the plasma of patients with acute lung injury (46). Recently, Walford *et al.* (47) have stated that hypoxia associated with tissue inflammation can modulate the effects of RNS on endothelial function and promotes the apoptotic cell death via peroxynitrite. Our data, from a different hypoxic/dysoxic model support these results. Our present findings, which show that Y-27632 decreases leukocyte infiltration and ROS/RNS mediated damage, may help to explain the potent, antiapoptotic effect exerted by rho

kinase inhibition in non-pulmonary sepsis-induced indirect acute lung injury.

Recently, it has been demostrated that statin therapy which is known to inhibit rho kinase pathway is associated with decreased mortality in bacteraemia (48,49). Statin use has been shown to attenuate the decline in lung function in the elderly patients during sepsis (50). The detailed mechanisms explained here for rho kinase pathway offer a plausible potential mechanism for such benefits, i.e. inhibition of sepsis driven apoptosis and ROS/RNS

mediated injury.

In conclusion, we have demonstrated an increased active fragmentation of ROCK 1 & 2, increased caspase 3 cleavage and increased production of peroxynitrite in lungs in a small animal model of sepsis. This was associated with significant lung injury as evidenced by increased apoptosis, increased permeability and lung edema, increased lung inflammation and histopathologic damage. All measured parameters of lung injury were ameliorated by Rho kinase inhibition. These findings emphasize the importance of the rho kinase pathway in sepsis-induced ROS and/or RNS-mediated, apoptosis-related lung injury. Inhibiting Rho kinase activation appears to be promising therapeutic principle for mitigating the development of indirect acute lung injury in sepsis as our data indicates that Rho kinase is positioned to regulate lung permeability, leukocyte trafficking, oxido-inflammatory pathways and apoptosis. The rho kinase pathway may represent a potential target for the future development of novel therapies in sepsis.

Acknowledgement

References

1.   Angus DC, Wax RS. Epidemiology of sepsis: an update. Crit Care Med 2001;29:S109-16.

2.   Cinel I, Dellinger RP. Advances in pathogenesis and management of sepsis. Curr Opin Infect Dis 2007;20:345-52.

3.   Cinel I, Opal SM. Molecular biology of inflammation and sepsis: a primer. Crit Care Med 2009;37:291-304.

4.   Hotchkiss RS, Swanson PE, Freeman BD, Tinsley KW, Cobb JP, Matuschak GM, et al. Apoptotic cell death in patients with sepsis, shock, and multiple organ dysfunction. Crit Care Med 1999;27:1230-51.

5.   Cinel I, Buyukafsar K, Cinel L, Polat A, Atici S, Tamer L, et al. The role of poly(ADP-ribose) synthetase inhibition in preventing endotoxemia-induced intestinal epithelial apoptosis. Pharmacol Res 2002;46:119-27.

6.   Bersten AD, Edibam C, Hunt T, Moran J. Incidence and mortality of acute lung injury and the acute respiratory distress syndrome in three Australian States. Am J Respir Crit Care Med 2002;165:443-8.

7.   Perl M, Chung CS, Perl U, Lomas-Neira J, de Paepe M, Cioffi WG, et al. Fas-induced pulmonary apoptosis and inflammation during indirect acute lung injury. Am J Respir Crit Care Med 2007;176:591-601.

8.   Hotchkiss RS, Karl IE. The pathophysiology and treatment of sepsis. N Engl J Med 2003;348:138-50.

9.   Ozdulger A, Cinel I, Koksel O, Cinel L, Avlan D, Unlu A, et al. The protective effect of N-acetylcysteine on apoptotic lung injury in cecal ligation and puncture-induced sepsis model. Shock 2003;19:366-72.

10. Hall A. Rho GTPases and the actin cytoskeleton. Science 1998;279:509-14.

11. Matsui T, Amano M, Yamamoto T, Chihara K, Nakafuku M, Ito M, et al. Rho-associated kinase, a novel serine/threonine kinase, as a putative target for small GTP binding protein Rho. EMBO J 1996;15:2208-16.

12. Riento K, Ridley AJ. Rocks: multifunctional kinases in cell behaviour. Nat Rev Mol Cell Biol 2003;4:446-56.

13. Fukata Y, Amano M, Kaibuchi K. Rho-Rho-kinase pathway in smooth muscle contraction and cytoskeletal reorganization of non-muscle cells. Trends Pharmacol Sci 2001;22:32-9.

14. Tasaka S, Koh H, Yamada W, Shimizu M, Ogawa Y, Hasegawa N, et al. Attenuation of endotoxin-induced acute lung injury by the Rho-associated kinase inhibitor, Y-27632. Am J Respir Cell Mol Biol 2005;32:504-10.

15. Ozaki M, Deshpande SS, Angkeow P, Bellan J, Lowenstein CJ, Dinauer MC, et al. Inhibition of the Rac1 GTPase protects against nonlethal ischemia/reperfusion-induced necrosis and apoptosis in vivo. FASEB J 2000;14:418-29.

16. Song Y, Hoang BQ, Chang DD. ROCK-II-induced membrane blebbing and chromatin condensation require actin cytoskeleton. Exp Cell Res 2002;278:45-52.

17. Shiotani S, Shimada M, Suehiro T, Soejima Y, Yosizumi T, Shimokawa H, et al. Involvement of Rho-kinase in cold ischemia-reperfusion injury after liver transplantation in rats. Transplantation 2004;78:375-82.

18. Arai M, Sasaki Y, Nozawa R. Inhibition by the protein kinase inhibitor HA1077 of the activation of NADPH oxidase in human neutrophils. Biochem Pharmacol 1993;46:1487-90.

19. Higashi M, Shimokawa H, Hattori T, Hiroki J, Mukai Y, Morikawa K, et al. Long-term inhibition of Rho-kinase suppresses angiotensin II-induced cardiovascular hypertrophy in rats in vivo: effect on endothelial NAD(P)H oxidase system. Circ Res 2003;93:767-75.

20. Coleman ML, Sahai EA, Yeo M, Bosch M, Dewar A, Olson MF. Membrane blebbing during apoptosis results from caspase-mediated activation of ROCK I. Nat Cell Biol 2001;3:339-45.

21. Morelli A, Chiozzi P, Chiesa A, Ferrari D, Sanz JM, Falzoni S, et al. Extracellular ATP causes ROCK I-dependent bleb formation in P2X7-transfected HEK293 cells. Mol Biol Cell 2003;14:2655-64.

22. Sebbagh M, Hamelin J, Bertoglio J, Solary E, Bréard J. Direct cleavage of ROCK II by granzyme B induces target cell membrane blebbing in a caspase-independent manner. J Exp Med 2005;201:465-71.

23. Ark M, Yilmaz N, Yazici G, Kubat H, Aktaş S. Rho-associated protein kinase II (rock II) expression in normal and preeclamptic human placentas. Placenta 2005;26:81-4.

24. Yagi K: Lipid peroxides and related radicals in clinical medicine. In: Armstrong D ed. Free Radicals in Diagnostic Medicine. Plenum Press New York 1994;pp 1-15.

25. Koksel O, Cinel I, Tamer L, Cinel L, Ozdulger A, Kanik A, et al. N-acetylcysteine inhibits peroxynitrite-mediated damage in oleic acid-induced lung injury. Pulm Pharmacol Ther 2004;17:263-70.

26. Koksel O, Yildirim C, Cinel L, Tamer L, Ozdulger A, Bastürk M, et al. Inhibition of poly(ADP-ribose) polymerase attenuates lung tissue damage after hind limb ischemia-reperfusion in rats. Pharmacol Res 2005;51:453-62.

27. LOWRY OH, ROSEBROUGH NJ, FARR AL, RANDALL RJ. Protein

measurement with the Folin phenol reagent. J Biol Chem 1951;193:265-75.

28. Breslin JW, Yuan SY. Involvement of RhoA and Rho kinase in neutrophil-stimulated endothelial hyperpermeability. Am J Physiol Heart Circ Physiol 2004;286:H1057-62.

29. Honing H, van den Berg TK, van der Pol SM, Dijkstra CD, van der Kammen RA, Collard JG, et al. RhoA activation promotes transendothelial migration of monocytes via ROCK. J Leukoc Biol 2004;75:523-8.

30. Saito H, Minamiya Y, Saito S, Ogawa J. Endothelial Rho and Rho kinase regulate neutrophil migration via endothelial myosin light chain phosphorylation. J Leukoc Biol 2002;72:829-36.

31. Thorlacius K, Slotta JE, Laschke MW, Wang Y, Menger MD, Jeppsson B, et al. Protective effect of fasudil, a Rho-kinase inhibitor, on chemokine expression, leukocyte recruitment, and hepatocellular apoptosis in septic liver injury. J Leukoc Biol 2006;79:923-31.

32. Breslin JW, Sun H, Xu W, Rodarte C, Moy AB, Wu MH, et al. Involvement of ROCK-mediated endothelial tension development in neutrophil-stimulated microvascular leakage. Am J Physiol Heart Circ Physiol 2006;290:H741-50.

33. Gorovoy M, Neamu R, Niu J, Vogel S, Predescu D, Miyoshi J, et al. RhoGDI-1 modulation of the activity of monomeric RhoGTPase RhoA regulates endothelial barrier function in mouse lungs. Circ Res 2007;101:50-8.

34. Cummings RJ, Parinandi NL, Zaiman A, Wang L, Usatyuk PV, Garcia JG, et al. Phospholipase D activation by sphingosine 1-phosphate regulates interleukin-8 secretion in human bronchial epithelial cells. J Biol Chem 2002;277:30227-35.

35. Zeng W, Matter WF, Yan SB, Um SL, Vlahos CJ, Liu L. Effect of drotrecogin alfa (activated) on human endothelial cell permeability and Rho kinase signaling. Crit Care Med 2004;32:S302-8.

36. Petrache I, Birukova A, Ramirez SI, Garcia JG, Verin AD. The role of the microtubules in tumor necrosis factor-alpha-induced endothelial cell permeability. Am J Respir Cell Mol Biol 2003;28:574-81.

37. Birukova AA, Birukov KG, Adyshev D, Usatyuk P, Natarajan V, Garcia JG, et al. Involvement of microtubules and Rho pathway in TGF-beta1-induced lung vascular barrier dysfunction. J Cell Physiol 2005;204:934-47.

38. Chiba Y, Ishii Y, Kitamura S, Sugiyama Y. Activation of rho is involved in the mechanism of hydrogen-peroxide-induced lung edema in isolated perfused rabbit lung. Microvasc Res 2001;62:164-71.

39. Thomas RA, Norman JC, Huynh TT, Williams B, Bolton SJ, Wardlaw AJ. Mechanical stretch has contrasting effects on mediator release from bronchial epithelial cells, with a rho-kinase-dependent component to the mechanotransduction pathway. Respir Med 2006;100:1588-97.

40. Lundblad C, Bentzer P, Grände PO. The permeability-reducing effects of prostacyclin and inhibition of Rho kinase do not counteract endotoxin-induced increase in permeability in cat skeletal muscle. Microvasc Res 2004;68:286-94.

41. Ho YS, Liou HB, Lin JK, Jeng JH, Pan MH, Lin YP, et al. Lipid peroxidation and cell death mechanisms in pulmonary epithelial cells induced by peroxynitrite and nitric oxide. Arch Toxicol 2002;76:484-93.

42. Salgo MG, Squadrito GL, Pryor WA. Peroxynitrite causes apoptosis in rat thymocytes. Biochem Biophys Res Commun 1995;215:1111-8.

43. Virág L, Scott GS, Cuzzocrea S, Marmer D, Salzman AL, Szabó C. Peroxynitrite-induced thymocyte apoptosis: the role of caspases and poly (ADP-ribose) synthetase (PARS) activation. Immunology 1998;94:345-55.

44. Chang J, Xie M, Shah VR, Schneider MD, Entman ML, Wei L, et al. Activation of Rho-associated coiled-coil protein kinase 1 (ROCK-1) by caspase-3 cleavage plays an essential role in cardiac myocyte apoptosis. Proc Natl Acad Sci U S A 2006;103:14495-500.

45. Bao F, Liu D. Peroxynitrite generated in the rat spinal cord induces apoptotic cell death and activates caspase-3. Neuroscience 2003;116:59-70.

46. Sittipunt C, Steinberg KP, Ruzinski JT, Myles C, Zhu S, Goodman RB, et al. Nitric oxide and nitrotyrosine in the lungs of patients with acute respiratory distress syndrome. Am J Respir Crit Care Med 2001;163:503-10.

47. Walford GA, Moussignac RL, Scribner AW, Loscalzo J, Leopold JA. Hypoxia potentiates nitric oxide-mediated apoptosis in endothelial cells via peroxynitrite-induced activation of mitochondria-dependent and -independent pathways. J Biol Chem 2004;279:4425-32.

48. Turner NA, O'Regan DJ, Ball SG, Porter KE. Simvastatin inhibits MMP-9 secretion from human saphenous vein smooth muscle cells by inhibiting the RhoA/ROCK pathway and reducing MMP-9 mRNA levels. FASEB J 2005;19:804-6.

49. Kruger P, Fitzsimmons K, Cook D, Jones M, Nimmo G. Statin therapy is associated with fewer deaths in patients with bacteraemia. Intensive Care Med 2006;32:75-9.

50. Alexeeff SE, Litonjua AA, Sparrow D, Vokonas PS, Schwartz J. Statin use reduces decline in lung function: VA Normative Aging Study. Am J Respir Crit Care Med 2007;176:742-7.